

Cardiomyocytes Derived from MHC-Homozygous Induced Pluripotent Stem Cells Exhibit Reduced Allogeneic Immunogenicity in MHC-Matched Non-human Primates

Takuji Kawamura,¹ Shigeru Miyagawa,¹ Satsuki Fukushima,¹ Akira Maeda,² Noriyuki Kashiyama,¹ Ai Kawamura,¹ Kenji Miki,³ Keisuke Okita,³ Yoshinori Yoshida,³ Takashi Shiina,⁴ Kazumasa Ogasawara,⁵ Shuji Miyagawa,² Koichi Toda,¹ Hiroomi Okuyama,² and Yoshiki Sawa^{1,*}

¹Department of Cardiovascular Surgery, Osaka University Graduate School of Medicine, Suita, Osaka 565-0871, Japan

²Department of Pediatric Surgery, Osaka University Graduate School of Medicine, Suita, Osaka 565-0871, Japan

³Department of Life Science Frontiers, Center for iPS Cell Research and Application, Kyoto University, Kyoto, Kyoto 606-8507, Japan

⁴Department of Molecular Life Science, Tokai University School of Medicine, Isehara, Kanagawa 259-1143, Japan

⁵Department of Pathology, Shiga University of Medical Science, Otsu, Shiga 520-2192, Japan

*Correspondence: sawa-p@surg1.med.osaka-u.ac.jp

<http://dx.doi.org/10.1016/j.stemcr.2016.01.012>

This is an open access article under the CC BY-NC-ND license (<http://creativecommons.org/licenses/by-nc-nd/4.0/>).

SUMMARY

Induced pluripotent stem cells (iPSCs) can serve as a source of cardiomyocytes (CMs) to treat end-stage heart failure; however, transplantation of genetically dissimilar iPSCs even within species (allogeneic) can induce immune rejection. We hypothesized that this might be limited by matching the major histocompatibility complex (MHC) antigens between the donor and the recipient. We therefore transplanted fluorescence-labeled (GFP) iPSC-CMs donated from a macaque with homozygous MHC haplotypes into the subcutaneous tissue and hearts of macaques having heterozygous MHC haplotypes (MHC-matched; group I) or without identical MHC alleles (group II) in conjunction with immune suppression. Group I displayed a higher GFP intensity and less immune-cell infiltration in the graft than group II. However, MHC-matched transplantation with single or no immune-suppressive drugs still induced a substantial host immune response to the graft. Thus, the immunogenicity of allogeneic iPSC-CMs was reduced by MHC-matched transplantation although a requirement for appropriate immune suppression was retained for successful engraftment.

INTRODUCTION

End-stage heart failure is generally characterized by an insufficient number of functional cardiomyocytes (CMs) (Towbin and Bowles, 2002). At this critical stage, cell transplantation is a promising approach for increasing the number of functional CMs. Thus, transplantation with induced pluripotent stem cells (iPSCs) represents a promising treatment for this condition (Yoshida and Yamanaka, 2010, 2011); accordingly, various studies have examined the potential application of iPSCs for cell transplantation therapy in the heart (Higuchi et al., 2015; Kawamura et al., 2012; Miki et al., 2012).

Cell transplantation therapy using iPSCs theoretically enables autologous transplantation, which could eliminate the need for immunosuppression and avoid related problems such as malignancy and infection. However, the clinical application of this approach is limited by safety concerns and high costs. To overcome the former limitation, banked iPSCs, in which safety has been established in advance, are under development with the aim of transplanting iPSC derivatives in an allogeneic fashion. However, this approach would inevitably induce the host immune response, limiting its therapeutic efficacy in turn.

Several approaches exist to prevent allogeneic cell transplantation-related immune rejection. One is immune sup-

pression therapy using a combination of several different types of immunosuppressants. Others are the use of major histocompatibility complex (MHC)-matched donor cells to reduce immunogenicity, or the suppression of MHC expression via genetic modification. MHC molecules function by binding to pathogen-derived peptide fragments and displaying them on their cell surface for T cell recognition; this process is affected by the high polymorphism of MHC genes. The recognition of non-self MHC molecules causes the rejection of allogeneic organs and tissues (Janeway et al., 2001); therefore, donor/recipient MHC matching can decrease the rate of rejection in organ transplantation (Flomenberg et al., 2004). For these approaches, the establishment of iPSC lines from healthy donors with homozygous MHC alleles is useful for minimizing the number of banked iPSC lines (Nakatsuji et al., 2008; Taylor et al., 2012).

The cynomolgus macaque is a non-human primate that is taxonomically more closely related to humans than other experimental primates. Cynomolgus macaques have a nearly identical genomic organization of the MHC region and drug metabolizing capacity similar to that of humans (Kita et al., 2009; Sano et al., 2006), thus making them a good model for organ transplantation and immunogenicity studies. At least 15 homozygous or semi-homozygous haplotypes (HT1–15) have



been identified in a Philippines macaque population (Shiina et al., 2015), with the most frequent haplotype, HT1, detected in 5%–10%.

In this study, we aimed to investigate the possibility of MHC-matched transplantation using this unique colony of primates, available through Ina Research Inc.. We hypothesized that iPSC-derived CMs (iPSC-CMs) with homozygous MHC haplotypes might prevent allogeneic immune rejection during MHC-matched transplantation.

RESULTS

MHC Genotyping

The results of MHC genotyping of iPSCs and seven macaque recipients are described in Table S1. The original macaque supplying the iPSCs expressed only one allele at all MHC gene loci except for the minor allele of A8*01:01, indicating that it carried a semi-homozygous MHC haplotype (termed HT1). Four macaques (nos. 1, 2, 6, and 7) carried all alleles constituting the HT1 haplotype and were used as MHC-matched recipients. In contrast, animals 3, 4, and 5 had no major HT1 haplotype alleles; these were used as MHC-mismatched recipients (Figure 1A).

Generation of iPSC-CMs

Undifferentiated macaque iPSCs expressed OCT4, TRA-1-60, and SSEA-4 (Figure S1A) and were differentiated to CMs under a protocol using human cytokines and chemicals (Figure 2A), which expressed CM marker genes with decreased OCT4 expression (Figure 2B). Nearly all of the aggregates showed self-beating (Movie S1) at day 10 and exhibited ~80% purity of troponin T, α actinin, and GFP-positive iPSC-CMs (Figures 2C and S1B).

The iPSC-CMs were seeded on temperature-responsive six-well dishes, and iPSC-CM sheets were collected at room temperature just before transplantation. The iPSC-CM sheet showed self-beating (Movie S2) and all cells therein expressed GFP (Figure 2I); approximately half of these cells expressed myosin light chain (MYL; Figure 2H) or myosin heavy chain (MYH; Figure 2I) as a CM marker. Flow cytometry indicated that 50% \pm 3% of the cell sheet population was positive for cardiac troponin T and 46% \pm 6% was positive for vimentin ($n = 5$) (Figures 2K and S1C), whereas CD31- or CD144-positive cells were rarely identified (Figure S1C). In addition, the vimentin-positive cells were located on the lower side of the cell sheet, which had attached to the dish (Figure 2J).

Reduced Expression of MHC Genes in iPSC-CMs

The expression of MHC class I genes in the iPSCs and after cardiomyogenic differentiation were relatively lower

compared with peripheral blood, although they were significantly increased following in vitro interferon- γ (IFN- γ) stimulation (Figure 2D). Mafa-E (*MHC-E*) expression was lowest among MHC class I genes (Figure 2E) and MHC class II genes were not expressed at any day of differentiation even following IFN- γ stimulation (data not shown).

Engraftment of iPSC-CMs in MHC-Matched Recipients

We first subcutaneously transplanted iPSC-CMs sheets into animals 1, 3, 6, and 7 to evaluate iPSC-CM sheet engraftment by quantitative GFP fluorescence evaluation at 2 weeks, 1 month, and 2 months after the transplantation (Figure 3A). GFP fluorescence could be detected in all groups at 2 weeks and 1 month. However, the fluorescence intensity was higher in HT1 heterozygous macaques treated with tacrolimus (TAC), mycophenolate mofetil (MMF), and prednisolone (PSL) (group I) than in the other groups at 1 month (Figure 3B). GFP fluorescence could not be detected at 2 months in recipient 3, which contained no HT1 alleles and was treated with TAC, MMF, and PSL (group II), or in HT1 heterozygous macaques treated with TAC only (group III) and untreated HT1 heterozygous macaques (group IV).

We next transplanted iPSC-CMs into the heart on the same day but prior to the subcutaneous transplantation in animals 2, 4, and 5 to investigate the engraftment of iPSC-CMs in the heart. The GFP fluorescence intensity in the subcutaneously transplanted graft of animal 2 at 1 or 2 months was higher than that of animal 4 or 5 (Figure 3A). The iPSC-CMs injected into the heart could be detected as GFP-positive cells in recipient 2 (group I) 2 months after the transplantation, but not in recipients 4 and 5 (group II) (Figures S2 and S3). The cells double-positive for GFP and MYH could be detected in recipient 2, although the number was limited (Figure S3).

Immunological Rejection of iPSC-CMs

To investigate the immunological rejection of transplanted iPSC-CMs, we histologically compared the subcutaneously transplanted iPSC-CMs (Figure 4) and quantified antibodies against iPSC-CMs in the serum at 1 month after transplantation (Figures S1F–S1I). Although serum levels of immunoglobulin M (IgM) or immunoglobulin G (IgG) against iPSC-CMs were not significantly increased compared with those at day 0, relatively severe infiltration of lymphocytes in the graft was histologically observed for all groups except group I. In detail, diffuse severe lymphocyte infiltration in nearly all parts of the grafts was observed in animals 3 and 7, and relatively localized severe infiltration around the vessels in the graft was observed in animals 4–6. On the other hand, in group I,

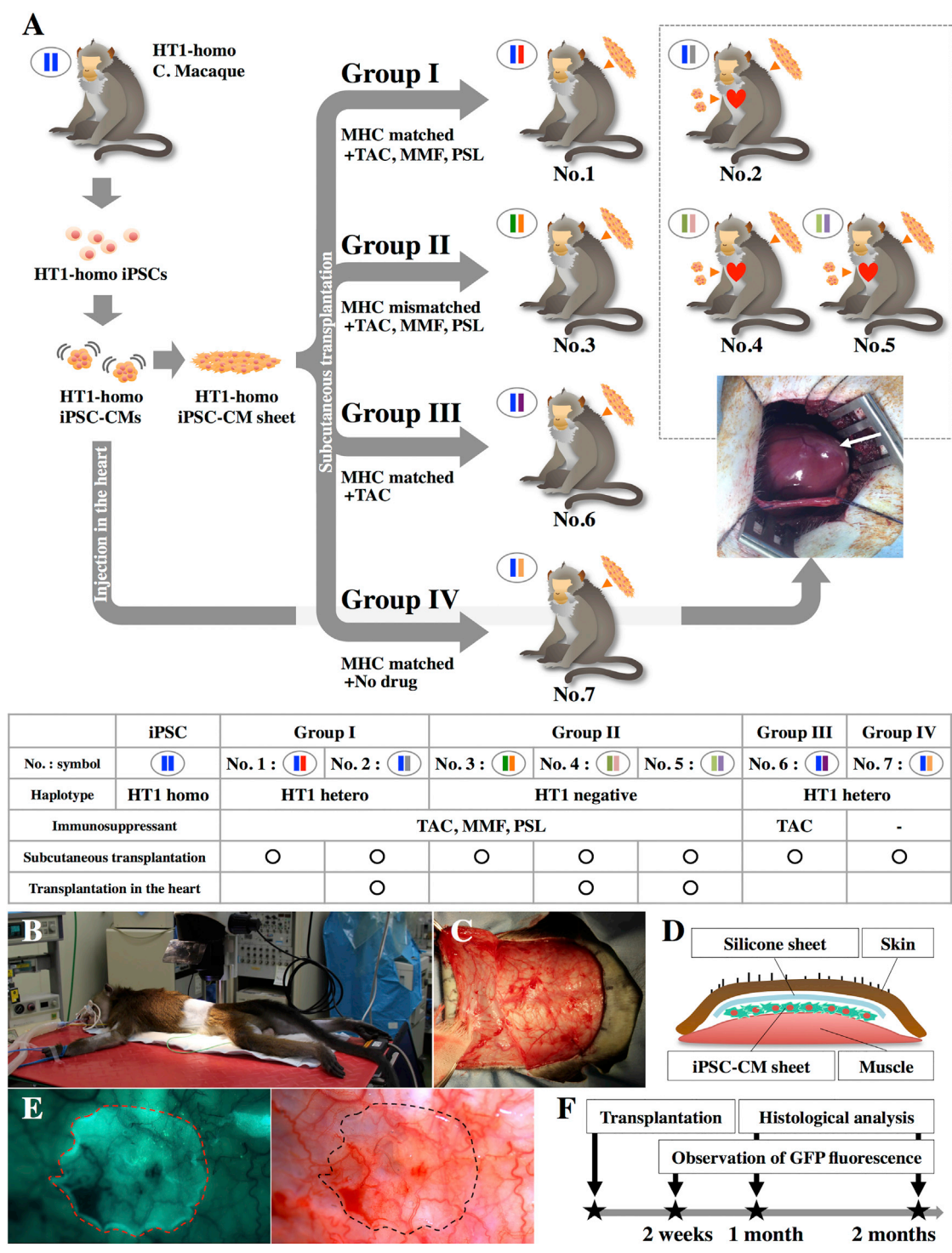


Figure 1. Subcutaneous Transplantation of an iPSC-CM Sheet into Cynomolgus Macaques

(A) Transplantation schema of HT1 homozygous (homo) iPSC-CMs.
 (B–D) Schema of subcutaneous transplantation of iPSC-CM sheets into the backs of recipient macaques. Hetero, heterozygous.
 (E) Observation of transplanted iPSC-CM sheets expressing GFP.
 (F) Follow-up examinations after iPSC-CM sheet transplantation.

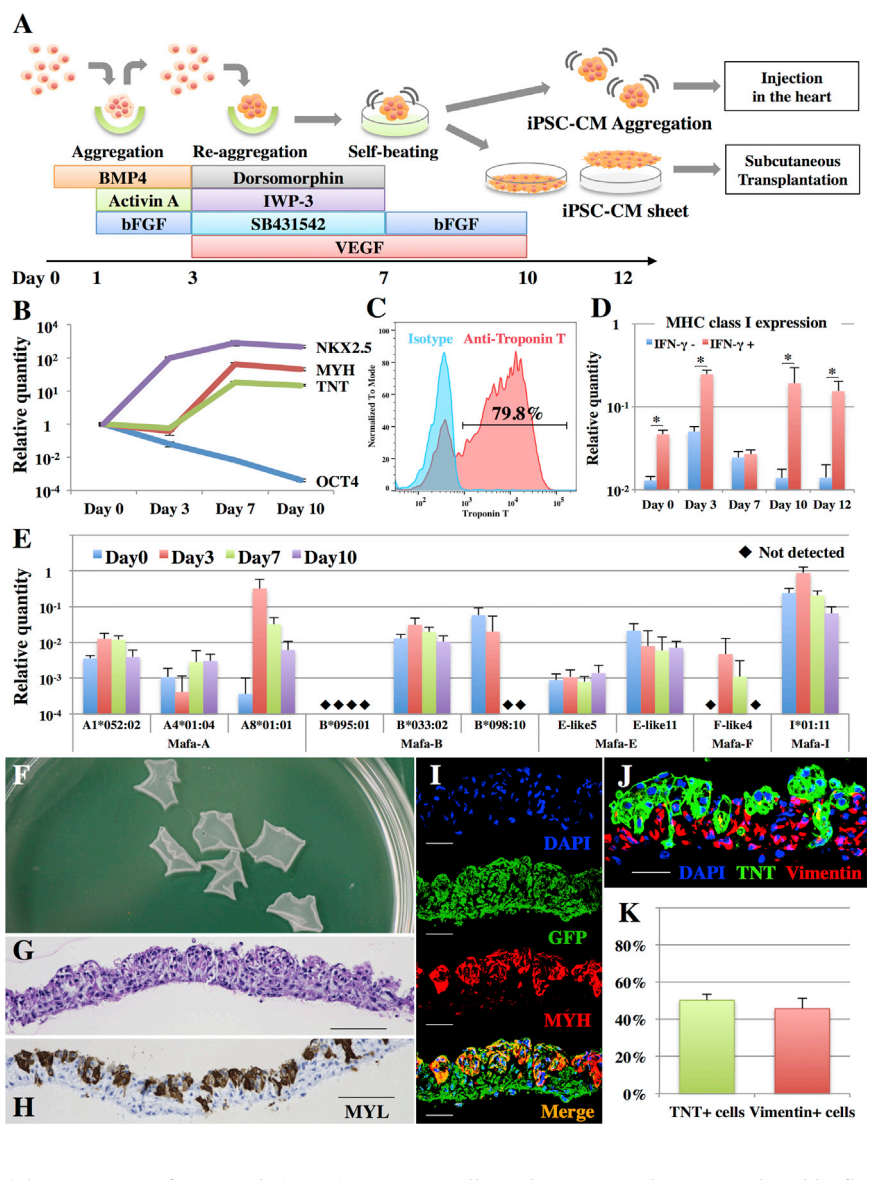


Figure 2. Generation of Cynomolgus Macaque iPSC-CM Sheets

(A) Cardiomyogenic differentiation protocol and the generation of iPSC-CM sheets. (B) Expression of NKX2.5, MYH, TNT, and OCT4 transcripts in iPSCs on days 0, 3, 7, and 10 as analyzed by real-time PCR. Results are relative to those at day 0 and are expressed as the means \pm SD (n = 3 independent experiments).

(C) Representative flow cytometry data of iPSC-CMs at day 10, stained with anti-troponin T antibodies or the isotype control. (D) Expression of MHC class I genes in iPSCs on days 0, 3, 7, 10, and 12 with or without IFN- γ stimulation as analyzed by real-time PCR. Results are relative to those of the peripheral blood and are expressed as the means \pm SD (n = 3 independent experiments). *p < 0.05.

(E) Expression of MHC class I genes in iPSCs on days 0, 3, 7, and 10 as analyzed by real-time PCR. *Mafa-A, B, F, E, and I* are the *MHC-A, B, F, E, and I* genes, respectively, in cynomolgus macaques. The relative quantities of each allele are compared with those of the peripheral blood and are expressed as the means \pm SD (n = 3 independent experiments). (F) Macaque iPSC-CM sheets in a 10-cm dish. (G) H&E staining of the iPSC-CM sheet. Scale bar, 100 μ m.

(H) Immunohistochemistry of MYL in the iPSC-CM sheet. Scale bar, 100 μ m. (I) Immunohistochemistry of GFP (Alexa Fluor 488), MYH (Alexa Fluor 546), and DAPI in the iPSC-CM sheet. Scale bar, 30 μ m. (J) Immunohistochemistry of TNT (Alexa Fluor 488), vimentin (Alexa Fluor 546), and DAPI in the iPSC-CM sheet. Scale bar, 30 μ m.

(K) Percentage of TNT- and vimentin-positive cells in the iPSC-CM sheet as analyzed by flow cytometry (representative data are shown in Figure S1C). Results are expressed as the means \pm SD (n = 5 independent experiments).

localized and relatively mild lymphocyte infiltration around the graft vessels was observed in animal 1, and almost none in animal 2. Semi-quantitative scoring for the number of CD3- or CD4-positive cells in the graft showed significantly lower numbers in the grafts of group I (CD3, 1,014/mm²; CD4, 531/mm²) compared with those of group II (CD3, 6,375/mm²; CD4, 3,950/mm²), whereas the values for group III (CD3, 5,810/mm²; CD4, 4,526/mm²) or group IV (CD3, 8,622/mm²; CD4, 3,805/mm²) were markedly higher (Figures 4B and S1D). Furthermore, the expression of interleukin-2 receptor (IL-2R) was decreased in group I grafts compared with the other groups (Figure S1E).

Natural Killer Cell-Related Rejection of iPSC-CMs

The low expression of MHC class I genes, including MHC-E in iPSC-CMs (Figure 2E) might cause natural killer (NK) cell-related immune reactions because HLA-E inhibits the cytotoxic activity of NK cells (Janeway et al., 2001). Therefore, we examined the number of NK cells in the subcutaneously transplanted iPSC-CMs by quantifying the expression of NK cell markers, i.e., immunoglobulin gamma Fc region receptor III (Fc γ R III) and natural killer group 2, member D (NKG2D). Their expression levels were increased in macaques not treated with immunosuppressants (group IV) or treated with TAC only (group III) compared with HT1 heterozygous

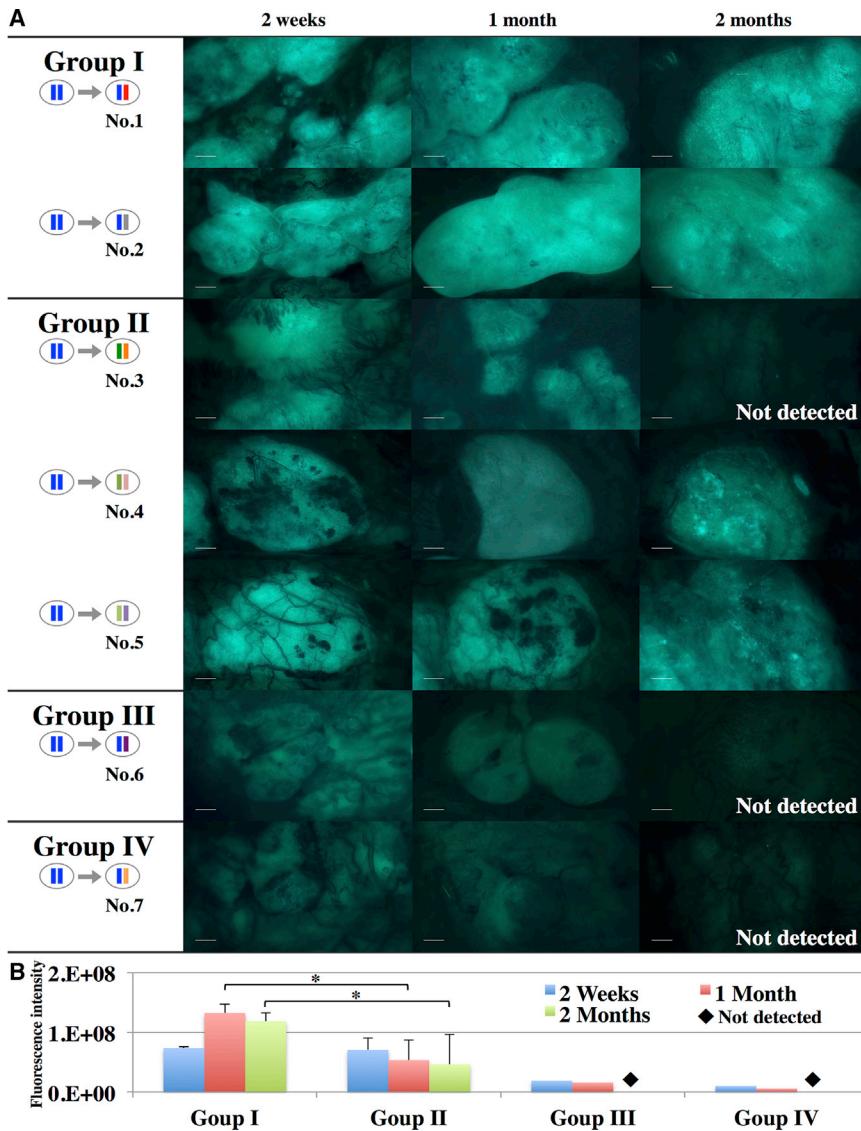


Figure 3. Engraftment of Subcutaneously Transplanted iPSC-CMs

(A) Images of subcutaneously transplanted iPSC-CMs expressing GFP obtained with a fluorescence stereomicroscope at 2 weeks, 1 month, and 2 months after transplantation. Scale bar, 2 mm.

(B) Quantification of the fluorescence intensity of GFP. Results are expressed as the means \pm SD for group I (nos. 1 and 2) and group II (nos. 3–5). * $p < 0.05$.

macaques treated with TAC, MMF, and PSL (group I) (Figure S1E).

DISCUSSION

In this study, we generated an iPSC line from the cynomolgus macaque with a homozygous MHC HT1 haplotype and obtained iPSC-CM cell sheets in which approximately one half of the cells were troponin T-positive CMs and the remainder were vimentin-positive cells; CD31- or CD144-positive cells were rarely identified. Because vimentin is an intermediate filament expressed in mesenchymal cells such as fibroblasts or endothelial cells, of which CD31 or CD144 is a marker, the vimentin-positive cells in the iPSC-CMs might possibly represent fibroblasts. Using

the iPSC-CMs, we provided evidence of the efficacy of MHC-matched allogeneic transplantation in a non-human primate model. Under the same TAC, MMF, and PSL immunosuppressive regimen, grafts in MHC-matched recipients showed significantly increased numbers of engrafted iPSC-CMs compared with those of MHC-mismatched recipients. Consistent with this, less severe infiltration of CD3+ and CD4+ T cells, suggestive of less severe rejection, were observed in MHC-matched recipients. However, all recipients regardless of MHC status exhibited severe rejection without appropriate immunosuppressants. These findings indicated that immunosuppressants in addition to TAC might be required to prevent rejection in MHC-matched iPSC-CM transplantation.

The efficacy and limitations of MHC-matched transplantation are related to the role of MHC in allogeneic cell

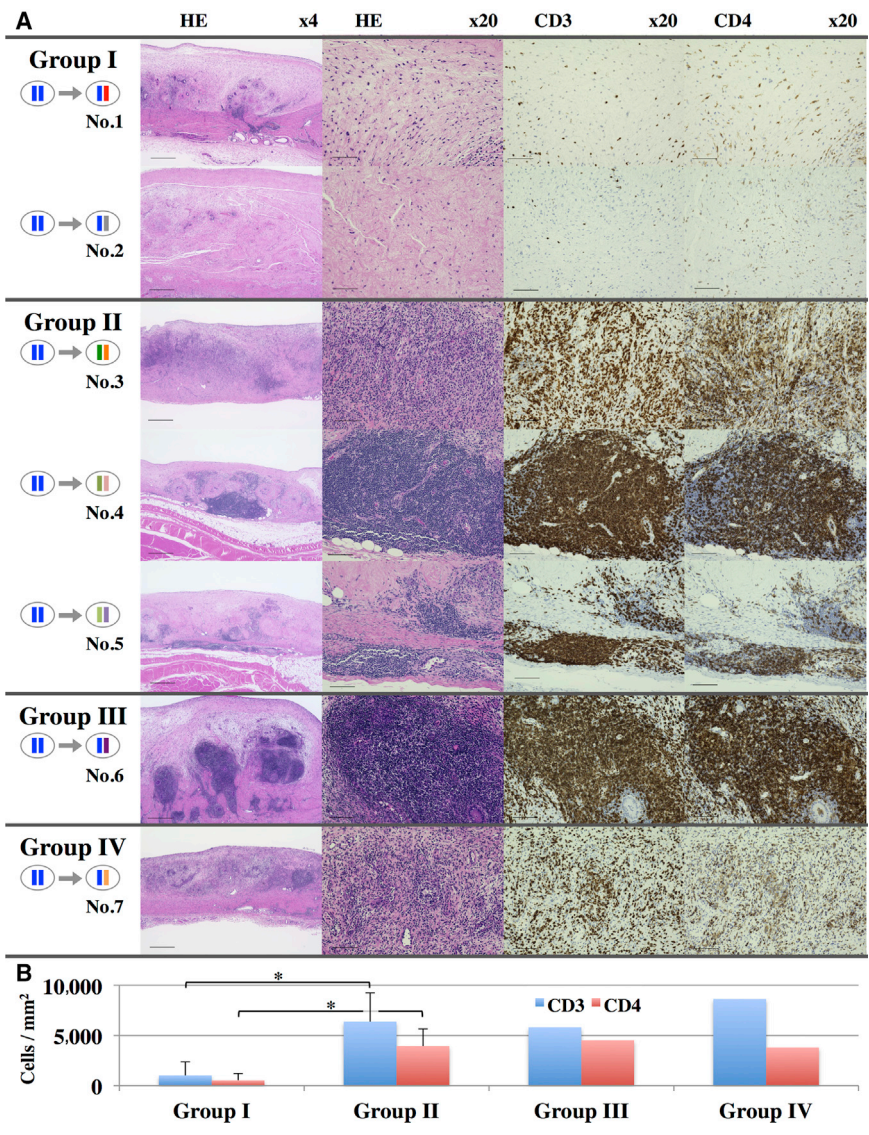


Figure 4. T Cell-Related Rejection of Transplanted iPSC-CMs

(A) H&E, CD3, or CD4 staining of the harvested iPSC-CM grafts 1 month after transplantation. Scale bars, 500 μm (4 \times), 100 μm (20 \times).

(B) Semi-quantitative scoring of the number of CD3- or CD4-positive cells in the graft 1 month after transplantation. The results are shown as the means \pm SD for group I (nos. 1 and 2) and group II (nos. 3–5). * $p < 0.05$.

transplantation. Theoretically, the main mechanism of MHC-matched transplantation is prevention of the host immune reaction through MHC-restricted direct recognition for the donor cells as self by the recipient immunocompetent cells, e.g., T cells. In general, approximately 1%–10% of naive T cells are activated by non-self MHC molecules, but not by self MHC molecules via such a “direct pathway” (Janeway et al., 2001). Therefore, MHC-matched transplantation might decrease the initial population of T cells activated by transplanted cell MHCs by recognizing them as self. In this study, the less severe rejection effected by MHC-matched versus mismatched iPSC-CM transplantation suggested that immune rejection via the direct pathway might have been minimal in the former. In addition, allogeneic iPSC-CMs caused severe rejection in MHC-mismatched transplantation with com-

bined immune suppression within 1 month, even though organ transplantation, including heart, lung, liver, and kidney transplantations, is usually performed in an MHC-mismatched manner without severe rejection under the appropriate immunosuppression therapy. Therefore, MHC-matched transplantation of iPSC-CMs represents a promising approach for clinical applications to avoid immunosuppression-related problems.

In contrast, MHC-matched transplantation might not have substantial effects on the prevention of allogeneic cell transplantation rejection in the indirect pathway, in which the transplanted cell antigens are presented after being phagocytosed and digested by recipient antigen-presenting cells to activate recipient T cells, as observed in animal 6 or 7. This might arise because the peptide antigens would be derived from MHC proteins and other non-self



peptides, acting as minor antigens. In this study, GFP might represent one of the minor antigens, as has previously been reported (Stripecke et al., 1999), or non-peptide antigens such as cell surface glycans, which have been reported to be highly expressed in iPSC-CMs (Kawamura et al., 2014, 2015), might serve as well. The antigen causing rejection in MHC-matched transplantation will need to be identified in further studies to overcome this limitation of allogeneic iPSC-CM transplantation.

Rejection might also have occurred as iPSC-CMs might fail to suppress recipient NK cells in MHC-matched transplantation. MHC class I molecules such as MHC-E, which are expressed on almost all cells in the body, bind to receptors on NK cells to inhibit cytotoxic activity and, following the immune reaction of NK cells (Janeway et al., 2001), are recognized as self. Since the expression levels of MHC class I genes in iPSC-CMs were low in this study, the grafts might have been recognized as non-self and rejected by recipient NK cells. Consistent with this, MHC-matched transplantation using TAC only or without immune suppressants induced elevated expression of the NK cell markers FcγR III and NKG2D in the grafts (Figure S1E), which might suggest that NK cell-related immune rejection might occur during MHC-matched iPSC-CM transplantation if the recipient did not receive appropriate immunosuppressants.

There were a few limitations to this study. The group sizes in this study were very small, which limits statistical robustness. In addition, we mainly performed subcutaneous transplantation of iPSC-CMs using silicone sheets to evaluate engraftment and rejection by direct observation of the transplanted iPSC-CMs and histological analysis of the grafts. This might not be the optimal location or the appropriate method as clinical applications would be expected to include transplantation to the heart without foreign material, which could provoke the host inflammatory response (Tang and Eaton, 1995) and might have worsened rejection. Notably, the iPSC-CMs transplanted into the heart in this study exhibited poorer survival compared with a previous report (Chong et al., 2014) in which human embryonic stem cell-derived cardiomyocytes were shown to survive for 3 months in the immune-suppressed macaque. This discrepancy might be due to the difference between the healthy heart in this study and the myocardial infarction model in the study of Chong et al., or might result from the different immunosuppressive regimens, both of which are expected to have a significant influence on the survival of transplanted cardiomyocytes. Further study would be needed for the detailed evaluation of immunological rejection and survival of the transplanted iPSC-CMs in disease model hearts according to the clinical applications.

In conclusion, the transplantation of MHC-matched iPSC-CMs was effective for preventing allogeneic immune

rejection and allowing engraftment of transplanted cells with appropriate immunosuppressants. The use of homozygous MHC banked iPSC lines might be useful for future regenerative therapy for a variety of pathologies.

EXPERIMENTAL PROCEDURES

Non-human Primates

Seven male cynomolgus macaques (Ina Research) were used in this study. Animal care procedures were consistent with the *Guide for the Care and Use of Laboratory Animals* (NIH). Experimental protocols were approved by the Ethics Review Committee for Animal Experimentation of Osaka University Graduate School of Medicine (reference no. 25-077-003).

Generation of iPSCs from Cynomolgus Macaques with Homozygous MHC

We used the cynomolgus macaque iPSC line, 1123C1-G (a gift from Professor Yamanaka), generated from an animal with a homozygous MHC haplotype as previously described (Okita et al., 2013). iPSCs were cultured using AK02 medium (Ajinomoto) on an LN511E8-coated (Nippi) dish as previously described (Miyazaki et al., 2012; Nakagawa et al., 2014). The iPSCs were then transfected with GFP as a donor cell marker as previously described (Morizane et al., 2013).

Cardiomyogenic Differentiation of Macaque iPSCs In Vitro

Cardiomyogenic differentiation of macaque iPSCs was performed using a previously described protocol (Miki et al., 2015) with modifications (Figure 2A, Supplemental Experimental Procedures). On day 12, the dish was incubated at room temperature, which induced the cells to detach from the dish forming scaffold-free iPSC-CM sheets.

Transplantation of iPSC-CMs

Transplantation was performed under general anesthesia, with intubation and ventilation using sevoflurane. Macaque iPSC-CM sheets, made from 3.3×10^6 cells per sheet, were subcutaneously transplanted into the backs of recipient animals (three sheets per animal). A 0.5-mm silicone sheet was placed on the iPSC-CM sheet to prevent its adhesion to the skin for repeat observations (Figures 1B–1E). In addition, injection of the iPSC-CMs into the heart was performed for animal 2, 4, and 5. The heart was exposed through left thoracotomy and iPSC-CM aggregations in PBS (approximately 3.3×10^6 cells) were delivered intramyocardially into the anterior wall of the left ventricle using an 18G needle. Needle tips were placed within a preformed mattress suture, which was closed to facilitate cell retention before needle withdrawal.

Immune Suppression

Macaques were divided into four groups as follows (Figure 1A): treated with TAC, MME, and PSL; treated with TAC only; given no immunosuppressants; and those with no HT1 alleles (MHC-mismatched allogeneic transplantation model) treated with TAC,



MMF, and PSL. Oral administration of 2 mg kg⁻¹ day⁻¹ TAC or continuous infusion of 0.5 mg kg⁻¹ day⁻¹ TAC to the femoral vein using an ALZET osmotic pump (DURECT Corp.) was performed from 2 days before transplantation to maintain serum trough levels at >10 ng ml⁻¹ until the end of the study. In addition, 40 mg kg⁻¹ day⁻¹ MMF and 1 mg kg⁻¹ day⁻¹ PSL were orally administered to the appropriate groups from 2 days before the transplantation until the end of the study. Drug dosages were based on clinical uses, as previously reported (Kinugasa et al., 2008; Song et al., 2014).

Quantitatively Observation of Transplanted iPSC-CMs

Transplanted iPSC-CM sheets were observed using a fluorescence stereomicroscope (MVX-10, Olympus) with fixed excitation laser intensity and identical exposure times. The GFP fluorescence intensities in the iPSC-CM sheets were quantified using ImageJ software as the green signal intensities standardized by subtracting the vessel intensities as the background and multiplied by the area. The GFP intensity correlation with cell number was confirmed by observing the two-layer and one-layer sections of the cell sheet on day 0 (Figure S4A).

SUPPLEMENTAL INFORMATION

Supplemental Information includes Supplemental Experimental Procedures, four figures, two tables, and two movies and can be found with this article online at <http://dx.doi.org/10.1016/j.stemcr.2016.01.012>.

AUTHOR CONTRIBUTIONS

T.K. provided study materials, collected and/or assembled the data, and wrote the manuscript; Shigeru M. provided financial support, and analyzed and interpreted the data; S.F., A.M., N.K., A.K., K.M., K. Okita, Y.Y., K.T., and H.O. analyzed and interpreted the data; T.S., K. Ogasawara, and Shuji M. conceived and designed the study, collected and/or assembled the data, and wrote the manuscript; Y.S. conceived and designed the study and provided financial support.

ACKNOWLEDGMENTS

We thank Professor Shinya Yamanaka of the Center for iPS Cell Research and Application, Kyoto University, who kindly provided the cynomolgus macaque iPSCs. We also thank Seiko Eiraku, Akima Harada, and Hiromi Nishinaka for their technical support. This study was supported by the Japan Science and Technology Agency as a part of the project, Center for the Development of Myocardial Regenerative Treatments Using iPS Cells.

Received: June 26, 2015

Revised: January 14, 2016

Accepted: January 15, 2016

Published: February 18, 2016

REFERENCES

Chong, J.J., Yang, X., Don, C.W., Minami, E., Liu, Y.W., Weyers, J.J., Mahoney, W.M., Van Biber, B., Palpant, N.J., Gantz, J.A., et al.

(2014). Human embryonic-stem-cell-derived cardiomyocytes regenerate non-human primate hearts. *Nature* 510, 273–277.

Flomenberg, N., Baxter-Lowe, L.A., Confer, D., Fernandez-Vina, M., Filipovich, A., Horowitz, M., Hurley, C., Kollman, C., Anasetti, C., Noreen, H., et al. (2004). Impact of HLA class I and class II high-resolution matching on outcomes of unrelated donor bone marrow transplantation: HLA-C mismatching is associated with a strong adverse effect on transplantation outcome. *Blood* 104, 1923–1930.

Higuchi, T., Miyagawa, S., Pearson, J.T., Fukushima, S., Saito, A., Tsuchimochi, H., Sonobe, T., Fujii, Y., Yagi, N., Astolfo, A., et al. (2015). Functional and electrical integration of induced pluripotent stem cell-derived cardiomyocytes in a myocardial infarction rat heart. *Cell Transplant.* 24, 2479–2489.

Janeway, C.A., Jr., Travers, P., Walport, M., and Shlomchik, M.J. (2001). *Immunobiology: The Immune System in Health and Disease*, Fifth edition (Garland Science).

Kawamura, M., Miyagawa, S., Miki, K., Saito, A., Fukushima, S., Higuchi, T., Kawamura, T., Kuratani, T., Daimon, T., Shimizu, T., et al. (2012). Feasibility, safety, and therapeutic efficacy of human induced pluripotent stem cell-derived cardiomyocyte sheets in a porcine ischemic cardiomyopathy model. *Circulation* 126, S29–S37.

Kawamura, T., Miyagawa, S., Fukushima, S., Yoshida, A., Kashiyama, N., Kawamura, A., Ito, E., Saito, A., Maeda, A., Eguchi, H., et al. (2014). N-Glycans: phenotypic homology and structural differences between myocardial cells and induced pluripotent stem cell-derived cardiomyocytes. *PLoS One* 9, e111064.

Kawamura, T., Miyagawa, S., Fukushima, S., Kashiyama, N., Kawamura, A., Ito, E., Saito, A., Maeda, A., Eguchi, H., Toda, K., et al. (2015). Structural changes in N-Glycans on induced pluripotent stem cells differentiating toward cardiomyocytes. *Stem Cells Transl. Med.* 4, 1258–1264.

Kinugasa, F., Nagatomi, I., Ishikawa, H., Nakanishi, T., Maeda, M., Hirose, J., Fukahori, H., Ooshima, S., Noto, T., Higashi, Y., et al. (2008). Efficacy of oral treatment with tacrolimus in the renal transplant model in cynomolgus monkeys. *J. Pharmacol. Sci.* 108, 529–534.

Kita, Y.F., Hosomichi, K., Kohara, S., Itoh, Y., Ogasawara, K., Tsuchiya, H., Torii, R., Inoko, H., Blancher, A., Kulski, J.K., et al. (2009). MHC class I A loci polymorphism and diversity in three Southeast Asian populations of cynomolgus macaque. *Immunogenetics* 61, 635–648.

Miki, K., Uenaka, H., Saito, A., Miyagawa, S., Sakaguchi, T., Higuchi, T., Shimizu, T., Okano, T., Yamanaka, S., and Sawa, Y. (2012). Bioengineered myocardium derived from induced pluripotent stem cells improves cardiac function and attenuates cardiac remodeling following chronic myocardial infarction in rats. *Stem Cells Transl. Med.* 1, 430–437.

Miki, K., Endo, K., Takahashi, S., Funakoshi, S., Takei, I., Katayama, S., Toyoda, T., Kotaka, M., Takaki, T., Umeda, M., et al. (2015). Efficient detection and purification of cell populations using synthetic MicroRNA switches. *Cell Stem Cell* 16, 699–711.

Miyazaki, T., Futaki, S., Suemori, H., Taniguchi, Y., Yamada, M., Kawasaki, M., Hayashi, M., Kumagai, H., Nakatsuji, N., Sekiguchi, K.,



- et al. (2012). Laminin E8 fragments support efficient adhesion and expansion of dissociated human pluripotent stem cells. *Nat. Commun.* 3, 1236.
- Morizane, A., Doi, D., Kikuchi, T., Okita, K., Hotta, A., Kawasaki, T., Hayashi, T., Onoe, H., Shiina, T., Yamanaka, S., et al. (2013). Direct comparison of autologous and allogeneic transplantation of iPSC-derived neural cells in the brain of a nonhuman primate. *Stem Cell Rep.* 1, 283–292.
- Nakagawa, M., Taniguchi, Y., Senda, S., Takizawa, N., Ichisaka, T., Asano, K., Morizane, A., Doi, D., Takahashi, J., Nishizawa, M., et al. (2014). A novel efficient feeder-free culture system for the derivation of human induced pluripotent stem cells. *Sci. Rep.* 4, 3594.
- Nakatsuji, N., Nakajima, F., and Tokunaga, K. (2008). HLA-haplotype banking and iPSC cells. *Nat. Biotechnol.* 26, 739–740.
- Okita, K., Yamakawa, T., Matsumura, Y., Sato, Y., Amano, N., Watanabe, A., Goshima, N., and Yamanaka, S. (2013). An efficient nonviral method to generate integration-free human-induced pluripotent stem cells from cord blood and peripheral blood cells. *Stem Cells* 31, 458–466.
- Sano, K., Shiina, T., Kohara, S., Yanagiya, K., Hosomichi, K., Shimizu, S., Anzai, T., Watanabe, A., Ogasawara, K., Torii, R., et al. (2006). Novel cynomolgus macaque MHC-DPB1 polymorphisms in three South-East Asian populations. *Tissue Antigens* 67, 297–306.
- Shiina, T., Yamada, Y., Aarnink, A., Suzuki, S., Masuya, A., Ito, S., Ido, D., Yamanaka, H., Iwatani, C., Tsuchiya, H., et al. (2015). Discovery of novel MHC-class I alleles and haplotypes in Filipino cynomolgus macaques (*Macaca fascicularis*) by pyrosequencing and Sanger sequencing: Mafa-class I polymorphism. *Immunogenetics* 67, 563–578.
- Song, L., Ma, A., Dun, H., Hu, Y., Zeng, L., Bai, J., Zhang, G., Kinugasa, F., Sudo, Y., Miyao, Y., et al. (2014). Effects of ASKP1240 combined with tacrolimus or mycophenolate mofetil on renal allograft survival in Cynomolgus monkeys. *Transplantation* 98, 267–276.
- Stripecke, R., Carmen Villacres, M., Skelton, D., Satake, N., Halene, S., and Kohn, D. (1999). Immune response to green fluorescent protein: implications for gene therapy. *Gene Ther.* 6, 1305–1312.
- Tang, L., and Eaton, J.W. (1995). Inflammatory responses to biomaterials. *Am. J. Clin. Pathol.* 103, 466–471.
- Taylor, C.J., Peacock, S., Chaudhry, A.N., Bradley, J.A., and Bolton, E.M. (2012). Generating an iPSC bank for HLA-matched tissue transplantation based on known donor and recipient HLA types. *Cell Stem Cell* 11, 147–152.
- Towbin, J.A., and Bowles, N.E. (2002). The failing heart. *Nature* 415, 227–233.
- Yoshida, Y., and Yamanaka, S. (2010). Recent stem cell advances: induced pluripotent stem cells for disease modeling and stem cell-based regeneration. *Circulation* 122, 80–87.
- Yoshida, Y., and Yamanaka, S. (2011). iPSC cells: a source of cardiac regeneration. *J. Mol. Cell Cardiol.* 50, 327–332.

Supplemental Information

**Cardiomyocytes Derived from MHC-Homozygous Induced Pluripotent
Stem Cells Exhibit Reduced Allogeneic Immunogenicity in MHC-
Matched Non-human Primates**

Takuji Kawamura, Shigeru Miyagawa, Satsuki Fukushima, Akira Maeda, Noriyuki Kashiyama, Ai Kawamura, Kenji Miki, Keisuke Okita, Yoshinori Yoshida, Takashi Shiina, Kazumasa Ogasawara, Shuji Miyagawa, Koichi Toda, Hiroomi Okuyama, and Yoshiki Sawa

Inventory of supplemental information

Figure S1. Cynomolgus Macaque iPSCs, iPSC-CMs and Transplanted iPSC-CM Rejection. Related to Figure 2, 4.

Figure S2. Rejection of Transplanted iPSC-CMs in the Heart. Related to Figures 3, 4.

Figure S3. Engraftment of Transplanted iPSC-CMs in the Heart. Related to Figures 3, 4.

Figure S4. Correlation of GFP Intensity with the Cell number and Positive Control for CD3 and CD4 Staining. Related to Figure 3B, 4

Movie S1. Beating cardiomyocytes derived from cynomolgus macaque iPSCs, related to Figure 2

Movie S2. Beating iPSC-CM sheet, related to Figure 2

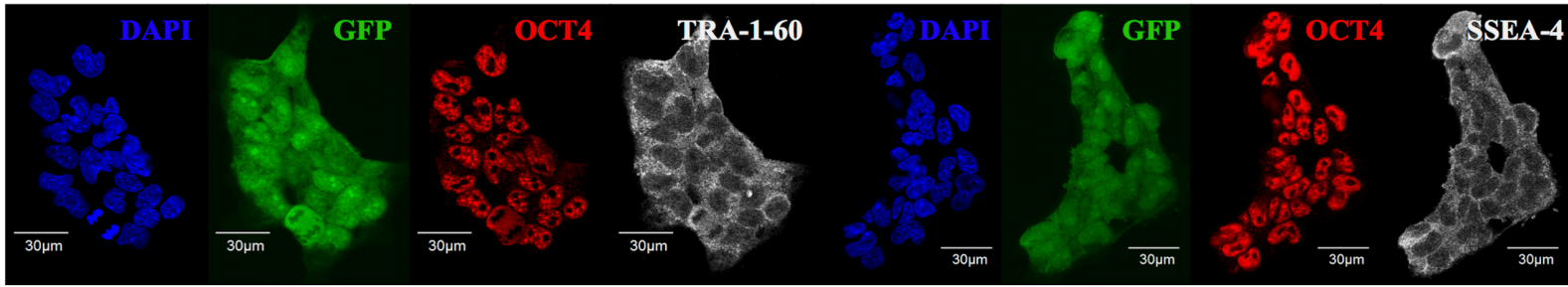
Table S1. MHC genotype, related to Figure 1

Table S2. Antibodies and Primers Used in This Study. Related to Figure 2, S1-4.

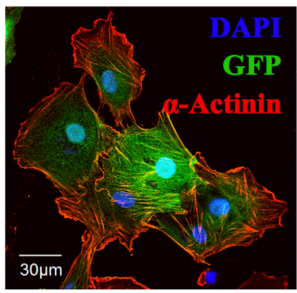
Supplemental experimental procedure

Figure S1

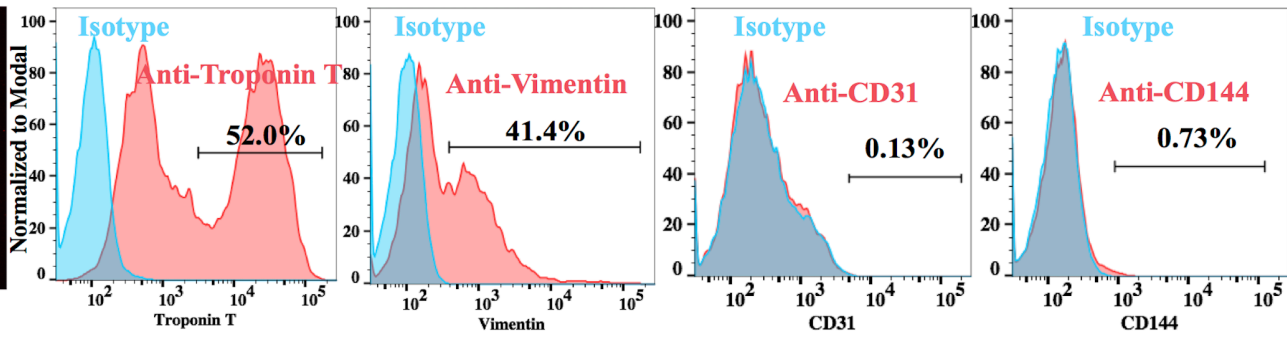
A



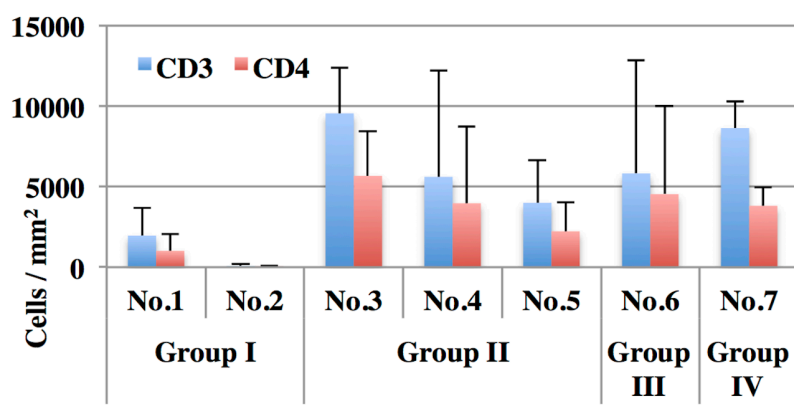
B



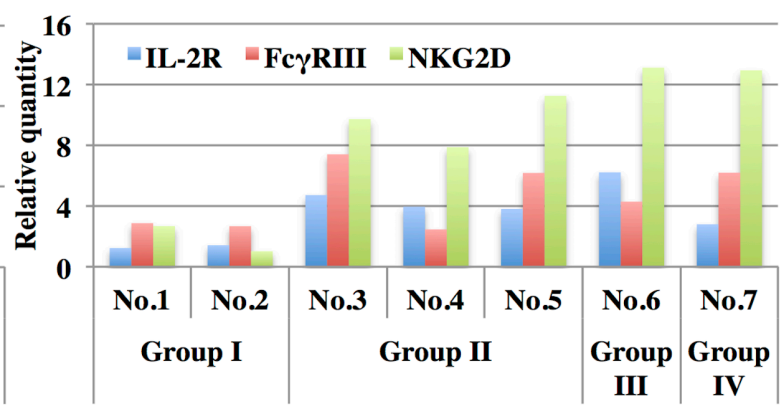
C



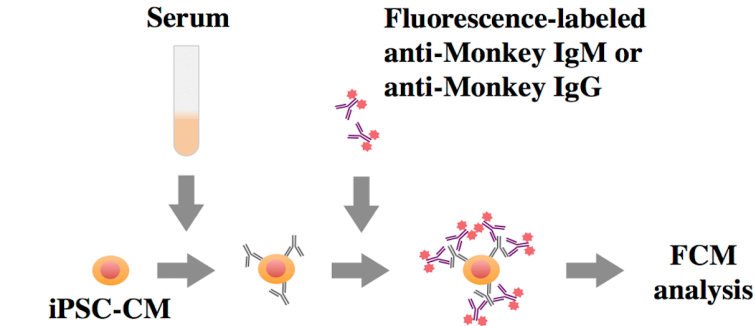
D



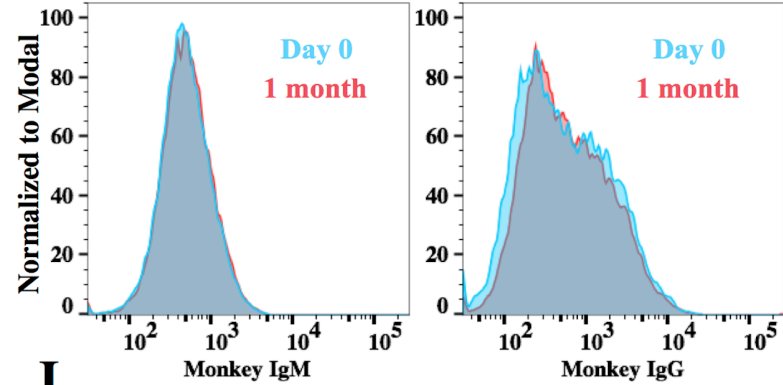
E



F



G



H



I

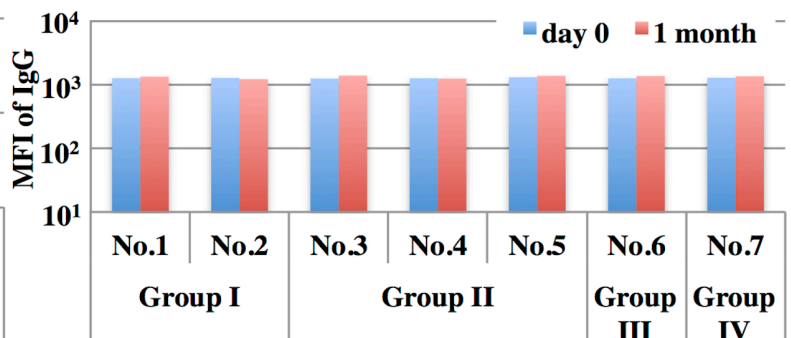
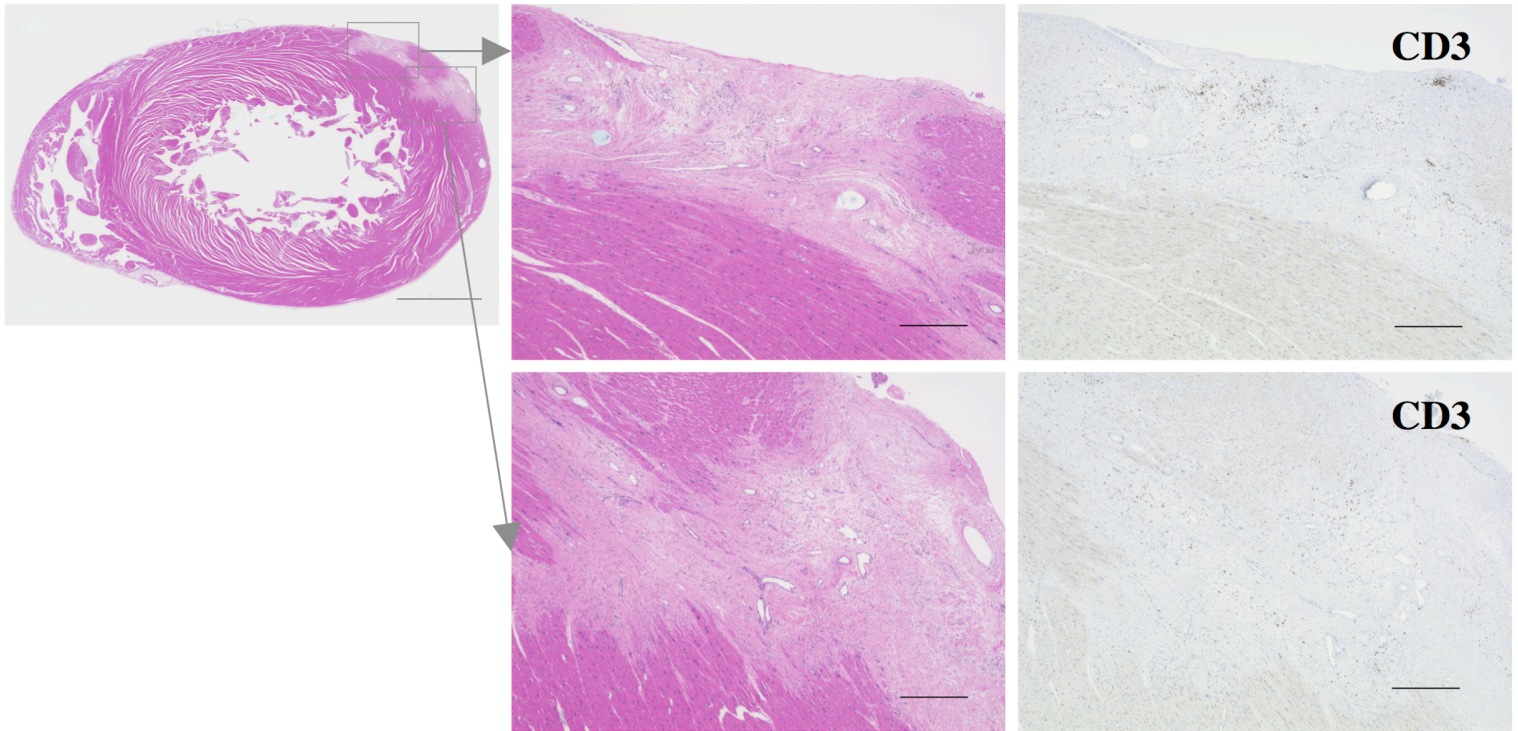
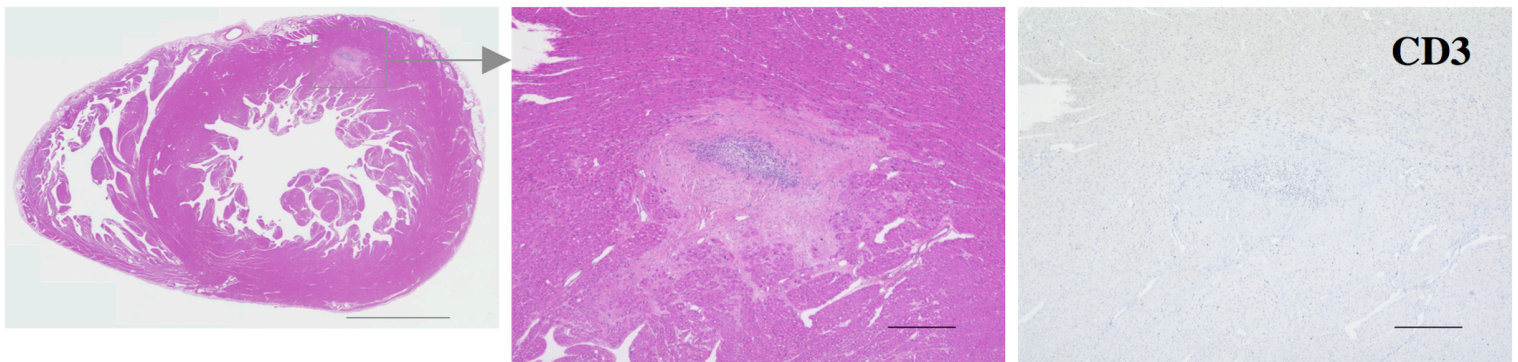


Figure S2

No.2 (II) → (II) **MHC-matched transplantation**



No.4 (II) → (III) **MHC-mismatched transplantation**



No.5 (II) → (III) **MHC-mismatched transplantation**

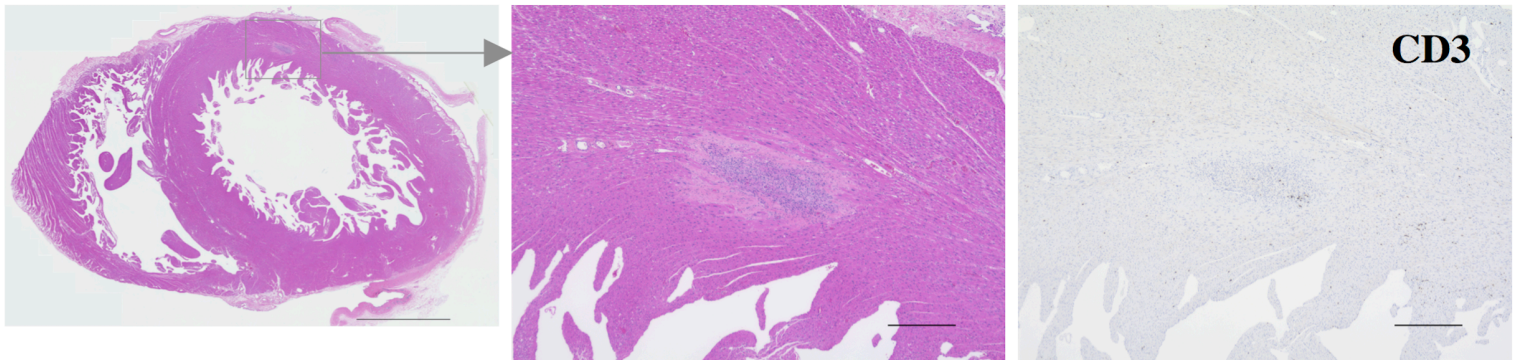

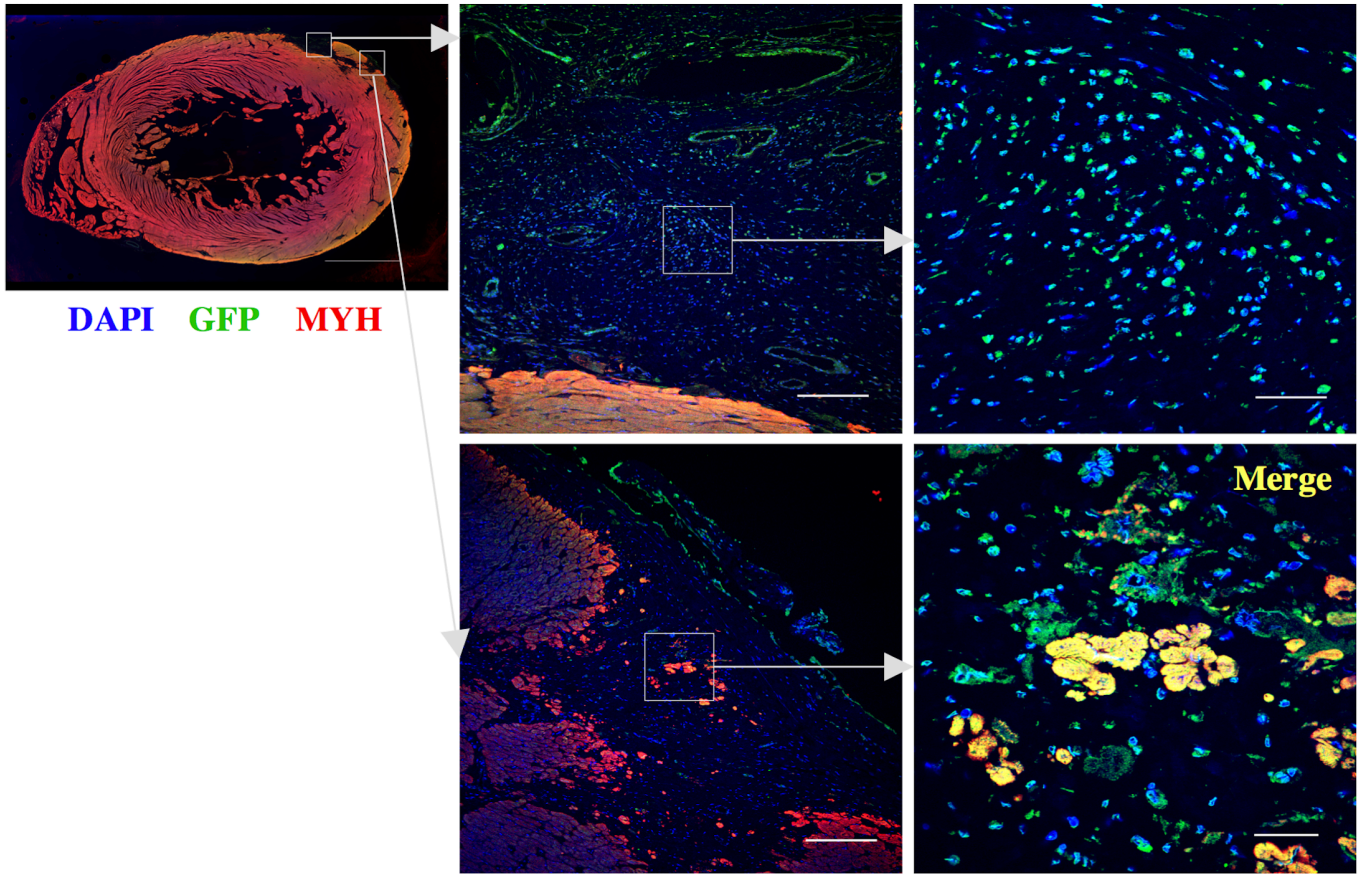

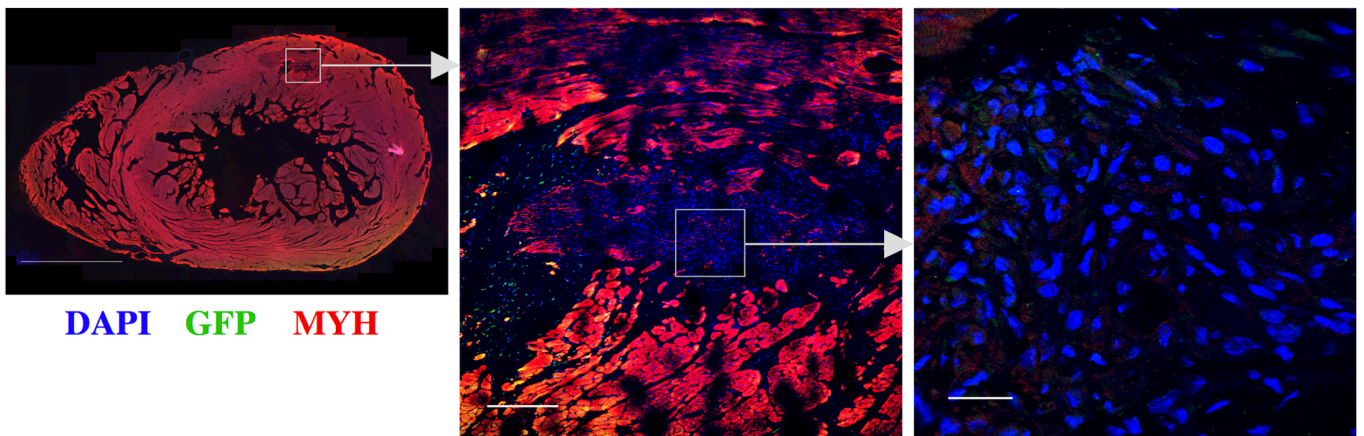


Figure S3

No.2  MHC-matched transplantation



No.4  MHC-mismatched transplantation



No.5  MHC-mismatched transplantation

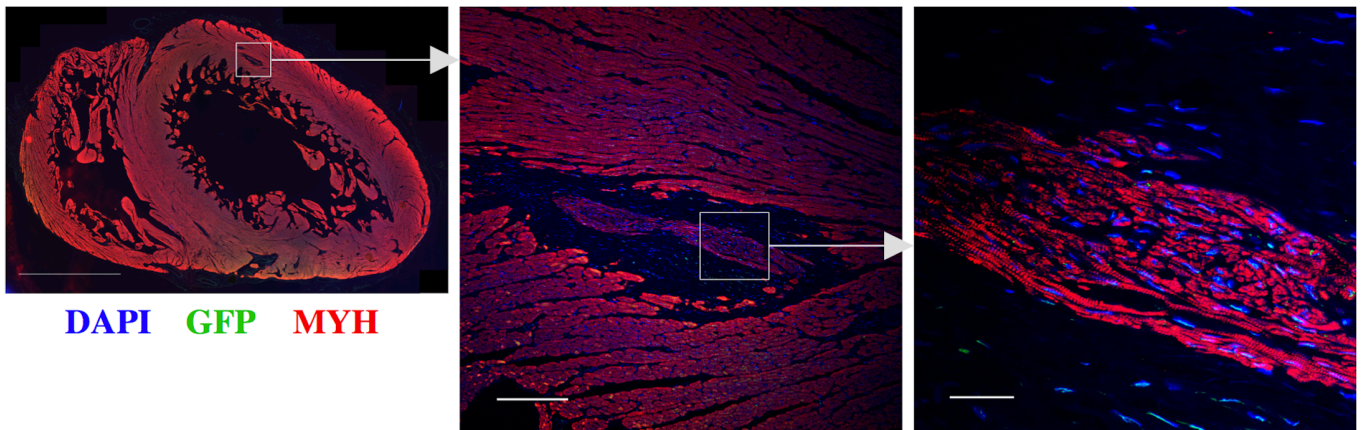
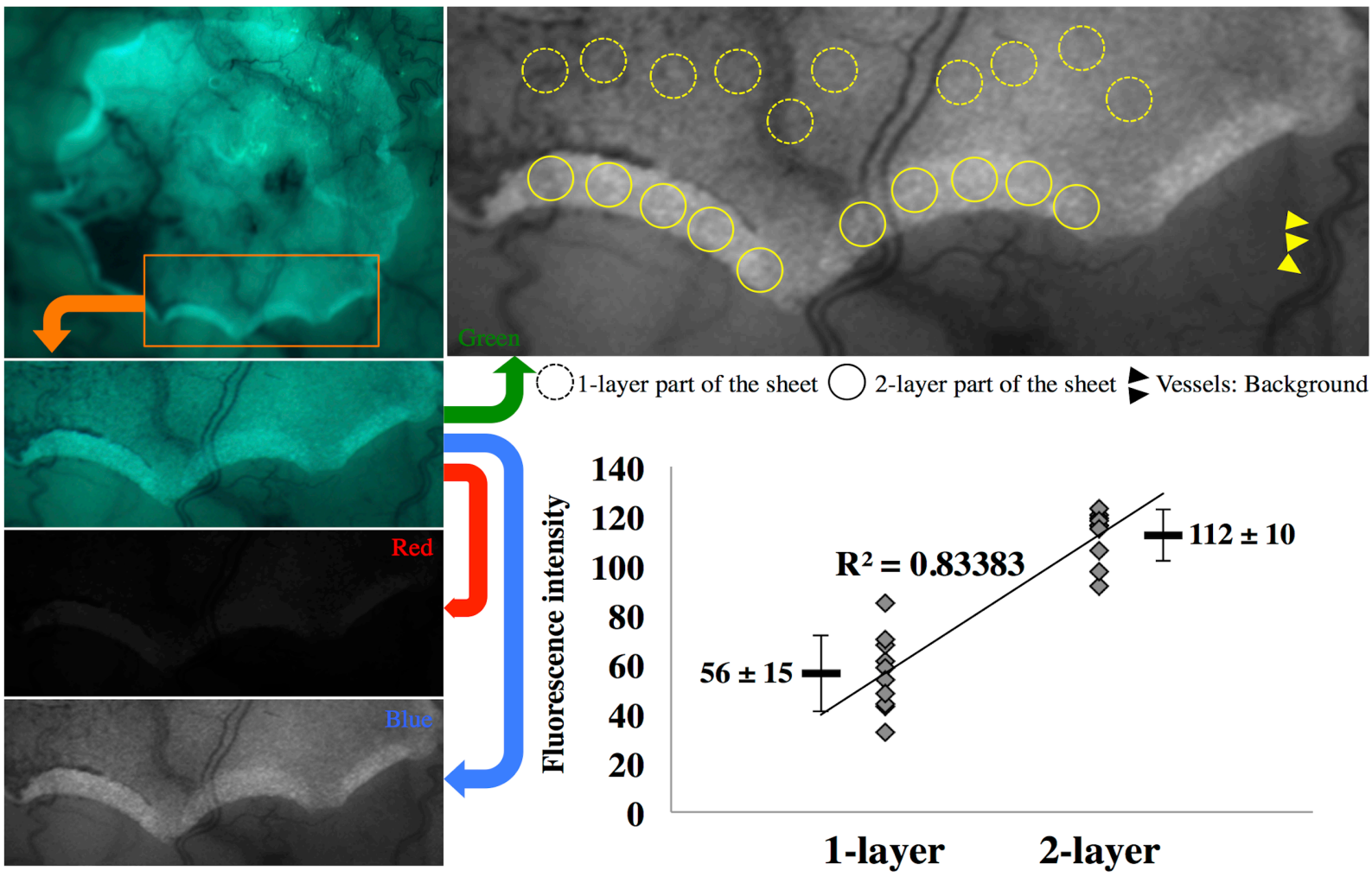


Figure S4

A



B

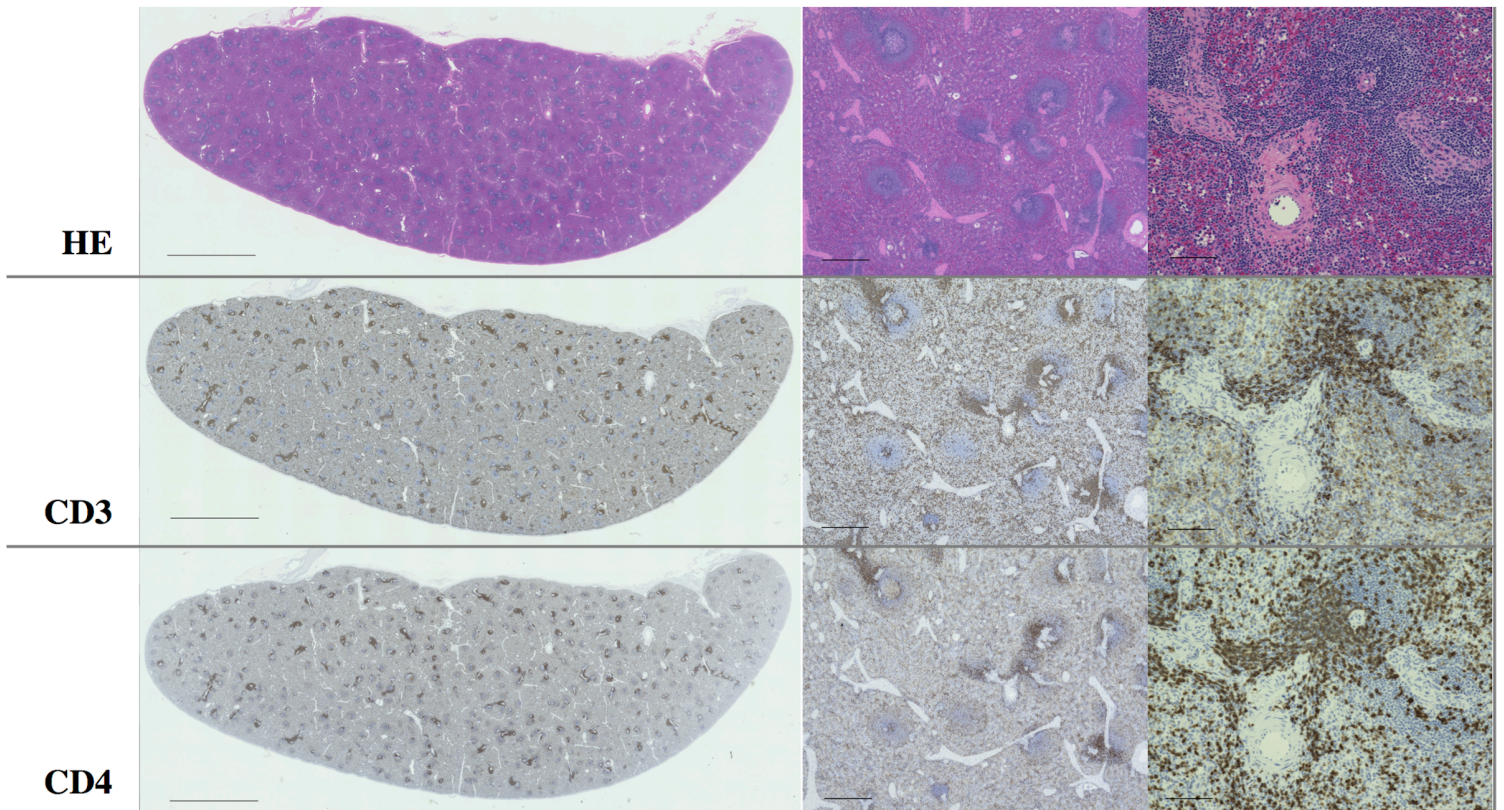


Table S1

Group	iPSC		Group I			Group II			Group III		Group IV		
	No. : symbol	No. 1 :	No. 2 :	No. 3 :	No. 4 :	No. 5 :	No. 6 :	No. 7 :	HTT1 hetero				
Haplotype	HTT1 near-homo		HTT1 hetero			HTT1 negative			HTT1 hetero				
Drug			TAC, MMF, PSL			TAC, MMF, PSL			TAC				
MHC class I	Mafra-A1	A1*052:02	A1*052:02	A1*052:02	A1*008:02	A1*089:03	A1*089:02	A1*089:03	A1*089:03	A1*089:03	A1*052:02	A1*052:02	A1*052:02
		A4*01:04	A4*01:04	A4*01:04	A1*086:02	A2*05:56	A2*05:50	A2*05:50	A2*05:50	A2*05:50	A4*01:04	A4*01:04	A4*01:04
	Mafra-A2-A8	A8*01:01	A8*01:01	A8*01:01		A3*13:03:01	A3*13:03:01	A3*13:03:01	A3*13:03:01	A3*13:03:01	A8*01:01	A3*13:03:01	A3*13:03:01
		B*095:01	B*095:01	B*095:01	B*066:02:01	B*137:03	B*104:03	B*159:01	B*091:02	B*160:01	B*095:01	B*095:01	B*095:01
		B*033:02	B*033:02	B*033:02	B*017:01	B*144:03N	B*144:03N	B*007:01:01	B*068:08	B*007:01:02	B*033:02	B*033:02	B*033:02
		B*098:10	B*098:10	B*098:10	B*157:01	B*057:04	B*057:04	B*158:01	B*070:05	B*070:05	B*098:10	B*098:10	B*098:10
	Mafra-B		B*098:11	B*098:11	B*050:08	B*060:02	B*060:02	B*115:04:02		B*098:09			
					B*060:02	B*046:01:02	B*046:01:02			B*158:01			
					B*116:01	B*050:08	B*050:08			B*085:01			
						B*114:02	B*114:02						
					B*072:01	B*072:01							
MHC class II	Mafra-E	E-like5	E-like5	E-like5	E-like3	E-like3	E-like2	E-like1	E-like1	E-like5	E-like3	E-like5	
		E-like11	E-like11	E-like11	E-like10	E-like10	E-like10			E-like11	E-like10	E-like11	
	Mafra-F	F-like4	F-like4	F-like4	F-like1	F-like1	F-like1	F-like2	F-like1	F-like4	F-like1	F-like4	F-like4
		I*01:11	I*01:11	I*01:10:02	I*01:10:01	I*01:18:02	I*01:12:01	I*01:11	I*01:14	I*01:11	I*01:13:01	I*01:11	I*01:11
	Mafra-DPA1	DPA1*02:05	DPA1*02:05	DPA1*07:02	DPA1*02:15:02	DPA1*04:02	DPA1*04:02	DPA1*07:04	DPA1*02:15:02	DPA1*07:04	DPA1*02:05	DPA1*07:04	DPA1*02:05
DPB1*15:04		DPB1*15:04	DPB1*19:03	DPB1*10:01	DPB1*03:04	DPB1*03:04	DPB1*21:01	DPB1*10:01	DPB1*21:01	DPB1*15:04	DPB1*21:01	DPB1*15:04	
Mafra-DQA1	DQA1*01:07:01	DQA1*01:07:01	DQA1*01:20	DQA1*26:03	DQA1*24:11	DQA1*26:03	DQA1*01:13	DQA1*26:03	DQA1*01:13	DQA1*01:07:01	DQA1*24:05	DQA1*01:07:01	
	DQB1*06:08	DQB1*06:08	DQB1*06:25	DQB1*18:07	DQB1*06:35	DQB1*18:07	DQB1*06:17:02	DQB1*18:07	DQB1*06:17:02	DQB1*06:08	DQB1*18:05	DQB1*06:08	
Mafra-DRB	DRB1*10:07	DRB1*10:07	DRB1*10:06	DRB*W1:08	DRB*W54:01	DRB*W1:08	DRB1*03:18	DRB*W33:02	DRB1*03:18	DRB1*10:07	DRB*W33:02	DRB1*10:07	
	DRB1*03:21	DRB1*03:21	DRB1*03:07	DRB*W36:01	DRB*W53:01	DRB*W36:01	DRB*W2:02	DRB*W36:01	DRB1*03:21	DRB1*03:21	DRB1*03:19	DRB*W3:01	
				DRB*W3:01		DRB*W3:01	DRB*W1:04		DRB*W1:04			DRB*W1:08	

Table S2

A

Antibodies	Source	Dilution
For immunocytochemistry and immunohistochemistry		
SSEA-4	Biologend, 330401	100
TRA-1-60	Biologend, 330602	100
OCT4	Abcam, ab19857	100
α -Actinin	Sigma-Aldrich, A7811	100
GFP	Abcam, ab290	200
MYL (myosin light chain)	Abcam, ab2480	200
MYH (myosin heavy chain)	Abcam, ab185967	200
TNT (troponin T)	Abcam, ab45932	200
Vimentin	Abcam, ab8978	200
CD3	NICHIREI BIOSCIENCES INC., 413591	1
CD4	NICHIREI BIOSCIENCES INC., 413181	1
For flow cytometry		
TNT (troponin T)	Thermo, #MS-295	100
Vimentin	Abcam, ab8978	100
CD31	BD Biosciences, 555446	100
CD144	BD Biosciences, 561567	100
Monkey IgM	LSBio, LS-C61219	100
Monkey IgG	LSBio, LS-C56744	100

B

Gene name	Primers (5'-3')
MHC-class I (monkey)	F: TCGTGCGGTTYGAYAGCGACG R: CCAGCA YCTCAGGGTGGCCTC
Oct4	F: GAGAACAATGAGAACCTTCAGGACA R: TTCTGGCGCCGGTTACAGAACCA
Nkx2.5	F: CCACCCACCCGTATTTATGTTT R: GGGGTCAACGCACTCTCTTT
MYH (myosin heavy chain)	F: CTGTACCAGAAGTCCTCCCTCAA R: TCTTGCCTCCTTTGCTTTTACC
TnT (troponin T)	F: TCTCCATCCTCTGCCTCACC R: CTGCTTCTTCCTGCTCCTCCT
IL-2R (interleukin-2 receptor)	F: TGAAGGGGTGCGATGGA R: AGTAGTGGGAGGCTTGGGAGA
NKG2D (natural-killer group 2, member D)	F: ATACAGCAAAGAGGACCAGGATTT R: AGTAGGTTGGGTGAGAGAATGGAG
Fc γ R III (immunoglobulin gamma Fc region receptor III)	F: TGGGTGTTCAAGGAGGAAGAA R: TGAGTGTGGCTTTTGGGAATGTAG
GAPDH (glyceraldehyde-3-phosphate dehydrogenase)	F: GAAGGTGAAGGTCGGAGTC R: CATTGATGGCAACAATATCC

SUPPLEMENTAL FIGURE LEGENDS

Figure S1. Cynomolgus Macaque iPSCs, iPSC-CMs and Transplanted iPSC-CM Rejection. Related to Figure 2, 4.

(A) Undifferentiated cynomolgus macaque iPSCs continuously expressing GFP stained with anti-OCT4 (Alexa Fluor 546), anti-TRA-1-60, or anti-SSEA-4 antibodies (Alexa Fluor 647) and DAPI. Scale bar, 30 μm . (B) iPSC-CMs at day 10, stained with anti- α -actinin antibodies (Alexa Fluor 546) and DAPI. Scale bar, 30 μm . (C) The cells in the iPSC-CM sheet, stained with anti-troponin T, anti-vimentin, anti-CD31, or anti-CD144 antibodies or the isotype control, analyzed with flow cytometry. (D) Semi-quantitative scoring for the number of CD3 or CD4 positive cells per mm^2 in the graft 1 month after transplantation are shown as the means \pm standard deviation for each animal. (randomly selected 10 views) (E) mRNA expression of Fc γ RIII, NKG2D, and IL-2R in the harvested iPSC-CM grafts 1 month after transplantation relative to those in normal subcutaneous tissue as analyzed by real-time PCR. The samples were harvested randomly from the graft ($n = 3$) and separately measured by triplicate experiments. The results are expressed as the means. (F) The schema for quantification of antibodies against iPSC-CMs (G) FCM analysis for anti-iPSC-CM IgM or IgG in the sera of No.1 macaque at day 0 and at 1 month after the transplantation. (H, I) Mean fluorescence intensity of iPSC-CMs, suspended in the serum of each macaque at day 0 and at 1 month after the transplantation, and subsequently stained with fluorescence labeled anti-monkey IgM (H) and IgG (I). Abbreviation: MFI, mean fluorescence intensity

Figure S2. Rejection of Transplanted iPSC-CMs in the Heart. Related to Figures 3, 4.

Hematoxylin-eosin (left) and CD3 staining of the heart (animal Nos. 2, 4, and 5) 2 months after iPSC-CM transplantation. Scale bars: 5 mm (left), 500 μm (middle and right).

Figure S3. Engraftment of Transplanted iPSC-CMs in the Heart. Related to Figures 3, 4.

The heart (animal Nos. 2, 4 and 5) 2 months after iPSC-CM transplantation stained by anti-GFP (Alexa Fluor 488) and anti-MYH antibodies (Alexa Fluor 546) and DAPI. Scale bars: 5 mm (left), 200 μm (middle), 30 μm (right).

Figure S4. Correlation of GFP Intensity with the Cell number and Positive Control for CD3 and CD4 Staining. Related to Figure 3B, 4.

(A) Observation of the cell sheet on day 0 of the transplantation was performed to confirm the correlation of GFP intensity with the cell number. Using Image J software, the image indicated in Figure 1E was split into 3 color files (Red, Blue, and Green). The intensities of green color in the solid circles within the 2-layer part of the cell sheet were about twice those in the dotted circles within the 1-layer and showed a high correlation (coefficient of determination: $R = 0.83383$). The result was expressed as the mean \pm standard deviation of indicated 10 circles. The green color intensities were standardized by

subtracting the intensities of the vessels as the background. (B) Hematoxylin-eosin staining and CD3 or CD4 staining of cynomolgus macaque spleens as a positive control. Scale bars: 5 mm (left), 500 μ m (middle), and 100 μ m (right).

SUPPLEMENTAL MOVIE LEGENDS

Movie S1. Beating Cardiomyocytes Derived from Cynomolgus Macaque iPSCs. Related to Figure 2.

Beating cell aggregations of cynomolgus macaque iPSCs at day 10 of cardiomyogenic differentiation at room temperature.

Movie S2. Beating iPSC-CM Sheet. Related to Figure 2.

A beating cynomolgus macaque iPSC-CM sheet at day 12 of cardiomyogenic differentiation at room temperature.

SUPPLEMENTAL TABLE LEGENDS

Table S1. MHC genotypes. Related to Figure 1.

MHC genotypes of iPSCs and the seven cynomolgus macaque recipients used in this study. The alleles constituting the HT1 haplotype are indicated by blue characters.

Table S2. Antibodies and Primers Used in This Study. Related to Figure 2.

Lists of (A) primary antibodies used for immunocytochemistry, immunohistochemistry, and flow cytometry and (B) primers for real-time PCR.

SUPPLEMENTAL EXPERIMENTAL PROCEDURES

Cardiomyogenic Differentiation Protocol

iPSCs (3×10^3) were resuspended in 70 μ l aliquots differentiation medium (DM; StemPro-34 [Invitrogen] containing 2 mM L-glutamine [Invitrogen], 30 mg/ml transferrin [Roche], 5 mg/ml ascorbic acid [Sigma], and 0.05 mg/ml 1-thioglycerol [Sigma]) containing 10 μ M Y-27632 (Rho-associated coiled-coil forming kinase inhibitor; Wako), 0.5% BD Matrigel Matrix Growth Factor Reduced (BD Biosciences), and 2 ng/ml recombinant human bone morphogenetic protein 4 (BMP4; R&D Systems) and cultured in 96-well Corning Costar Ultra-Low attachment multiwell plates (Sigma-Aldrich). On day 1, an additional 70 μ l DM containing 18 ng/ml BMP4, 10 ng/ml recombinant human fibroblast growth factor basic (bFGF; R&D Systems), and 12 ng/ml recombinant human activin A (R&D Systems) was added to each well. On day 3, the aggregates were enzymatically digested to single cells, and 1×10^4 cells were resuspended in 100 μ l aliquots DM containing 10 ng/ml recombinant human vascular endothelial growth factor (VEGF; R&D Systems), 1 μ M IWP-3 (Wnt signaling inhibitor; Stemolecule), 5.4 μ M SB431542 (transforming growth factor- β signaling inhibitor; Sigma-Aldrich), and 0.6 μ M dorsomorphin (BMP signaling inhibitor; Sigma-Aldrich) and cultured in 96-well Corning Costar Ultra-Low attachment multiwell plates (Sigma-Aldrich). On day 7, individual cell aggregates were transferred to 24-well Corning Costar Ultra-Low attachment multiwell plates (Sigma-Aldrich; 10 aggregates per well) in DM containing 10 ng/ml VEGF (R&D Systems) and 5 ng/ml bFGF (R&D Systems). From day 0 to 10, the cells were incubated at 37°C in a hypoxic atmosphere (5% O₂) with 5% CO₂ using a HERAcell CO₂ incubator (Thermo Fisher Scientific). On day 10, the aggregates were enzymatically digested to single cells and 3.3×10^6 cells were seeded onto 6-well UpCell dishes (temperature-responsive dishes; CellSeed) and incubated at 37°C in a normoxic atmosphere with 5% CO₂. On day 12, the dish was incubated at room temperature, which caused the cells to detach spontaneously to form scaffold-free cynomolgus macaque iPSC-derived cardiomyocyte sheets.

Immunocytochemistry Analysis

Cynomolgus macaque iPSCs and iPSC-CMs were fixed with 4% paraformaldehyde and stained with the listed primary antibodies (Table S2A). Cell nuclei were stained with 4',6-diamidino-2-phenylindole dihydrochloride (DAPI) and observed with the confocal laser scanning microscope FV1200 (Olympus).

Flow Cytometry

iPSC-CMs were dissociated with 0.25% trypsin-EDTA and then fixed with CytoFix fixation buffer (BD Biosciences). The cells were stained with mouse anti-troponin T antibodies (Thermo) or anti-vimentin antibodies (Abcam) in Perm/Wash buffer (BD Biosciences) and visualized with Alexa Fluor 647 rabbit anti-mouse IgG (Invitrogen), or stained with phycoerythrin conjugated anti-CD31 antibodies (BD Biosciences) or Alexa Fluor 647 conjugated anti-CD144 antibodies (BD Biosciences).

The labeled cells were analyzed on a FACS Canto II (BD Biosciences). All data were analyzed in five independent experiments.

Immunohistochemistry Analysis

iPSC-CM sheets, harvested iPSC-CM grafts, and the hearts were fixed with 4% paraformaldehyde, embedded in paraffin, and sectioned. The heart samples of animals 2, 4, and 5 were obtained by cutting the heart laterally at the point in which the iPSC-CMs had been injected and sectioning. After antigen retrieval by heating in ethylenediaminetetraacetic acid and endogenous peroxidase deactivation with 3% H₂O₂, the sections were stained with the listed antibodies (Table S2A) and horseradish peroxidase-labeled polymer (Nichirei Biosciences, Inc.), followed by 3,3'-diaminobenzidine (DAB) color development, or fluorescence labeled secondary antibodies, as appropriate.

Semi-quantitative scoring for the number of the CD3 or CD4 positive cells in the grafts

CD3 or CD4 positive cells in the grafts were counted on the DAB color stained sample. The number of DAB color positive cells were automatically counted with a microscope and its software (BZ-X700, KEYENCE, Osaka, Japan) from randomly selected 10 views in each sample. The result was expressed as the mean \pm standard deviation for each animal. CD3 and CD4 staining was confirmed using cynomolgus macaque spleens as a positive control (Figure S4B).

Quantification of Antibodies against iPSC-CMs

iPSC-CMs were suspended in 10% diluted serum obtained from the macaques at day 0 or at 1 month after the transplantation. Subsequently, the cells were stained with a Texas Red-conjugated goat anti-monkey IgM antibody or a fluorescein isothiocyanate-conjugated goat anti-monkey IgG antibody (LSBio) (Figure S3). Fluorescence intensities were measured by a FACSCanto II instrument (BD Biosciences). Dead cells were excluded after staining with the LIVE/DEAD[®] Fixable Violet Dead Cell Stain Kit (Invitrogen) according to the manufacturer's recommended protocol.

Semi-quantitative Polymerase Chain Reaction (PCR)

DNA-free total RNA was extracted with an RNeasy RNA isolation Kit (Qiagen), reverse-transcribed into cDNA using Omniscript reverse transcriptase (Qiagen), and analyzed by quantitative real-time PCR on an ABI PRISM 7700 thermocycler (Applied Biosystems) with SYBR Green dye (Applied Biosystems) using the listed primers (Table S2B). All data were analyzed by the relative standard curve method in three independent experiments in triplicate.

Genotyping of MHC

MHC genotyping was performed as previously described (Morizane et al., 2013). Briefly, total RNA was isolated from the

peripheral white blood cells using TRIzol (Invitrogen). cDNA was synthesized using ReverTra Ace (TOYOBO). The MHC class I gene primer pairs used for macaque genes were designed based on generic sequences in exons 2 to 4 that amplify all known class I genes. After RT-PCR amplification using high fidelity KOD FX polymerase (TOYOBO), pyrosequencing of the PCR products was carried out using the GS Junior system and amplicon sequencing protocol (Roche). MHC genotypes were assigned by comparing the sequences to known MHC allele sequences released from the Immuno Polymorphism Database.

Statistical Analysis

Data are reported as the means \pm standard deviation and were compared using Student's t-tests. Differences with p-values of less than 0.05 were considered statistically significant. All statistical analyses were performed using JMP 11.0 (SAS Institute).